Biomedical Optics EXPRESS

Label-free near-infrared reflectance microscopy as a complimentary tool for two-photon fluorescence brain imaging

Anna Letizia Allegra Mascaro,[1,2,*] Irene Costantini,[1] Emilia Margoni,[1] Giulio Iannello,[3] Alessandro Bria,[3,4] Leonardo Sacconi,[1,2] and Francesco S. Pavone[1,2,5]

[1]*European Laboratory for Non-Linear Spectroscopy, University of Florence, Via Nello Carrara 1, Sesto Fiorentino 50019, Italy*
[2]*National Research Council, National Institute of Optics, Largo Fermi 6, Florence 50125, Italy*
[3]*Department of Engineering, Università Campus Bio-Medico di Roma, 00128 Rome, Italy*
[4]*Department of Electrical and Information Engineering, University of Cassino and L. M. Italy*
[5]*University of Florence, Department of Physics and Astronomy, Via Sansone 1, Sesto Fiorentino 50019, Italy*
[*]*allegra@lens.unifi.it*

Abstract: *In vivo* two-photon imaging combined with targeted fluorescent indicators is currently extensively used for attaining critical insights into brain functionality and structural plasticity. Additional information might be gained from back-scattered photons from the near-infrared (NIR) laser without introducing any exogenous labelling. Here, we describe a complimentary and versatile approach that, by collecting the reflected NIR light, provides structural details on axons and blood vessels in the brain, both in fixed samples and in live animals under a cranial window. Indeed, by combining NIR reflectance and two-photon imaging of a slice of hippocampus from a Thy1-GFPm mouse, we show the presence of randomly oriented axons intermingled with sparsely fluorescent neuronal processes. The back-scattered photons guide the contextualization of the fluorescence structure within brain atlas thanks to the recognition of characteristic hippocampal structures. Interestingly, NIR reflectance microscopy allowed the label-free detection of axonal elongations over the superficial layers of mouse cortex under a cranial window in vivo. Finally, blood flow can be measured in live preparations, thus validating label free NIR reflectance as a tool for monitoring hemodynamic fluctuations. The prospective versatility of this label-free technique complimentary to two-photon fluorescence microscopy is demonstrated in a mouse model of photothrombotic stroke in which the axonal degeneration and blood flow remodeling can be investigated.

OCIS codes: (170.0110) Imaging systems; (170.3880) Medical and biological imaging.

References and links

1. A. J. Canty, L. Huang, J. S. Jackson, G. E. Little, G. Knott, B. Maco, and V. De Paola, "In-vivo single neuron axotomy triggers axon regeneration to restore synaptic density in specific cortical circuits," Nat. Commun. **4**, 2038 (2013).
2. A. L. Allegra Mascaro, P. Cesare, L. Sacconi, G. Grasselli, G. Mandolesi, B. Maco, G. W. Knott, L. Huang, V. De Paola, P. Strata, and F. S. Pavone, "In vivo single branch axotomy induces GAP-43-dependent sprouting and synaptic remodeling in cerebellar cortex," Proc. Natl. Acad. Sci. U.S.A. **110**(26), 10824–10829 (2013).
3. A. Holtmaat and K. Svoboda, "Experience-dependent structural synaptic plasticity in the mammalian brain," Nat. Rev. Neurosci. **10**(9), 647–658 (2009).
4. A. Holtmaat, J. Randall, and M. Cane, "Optical imaging of structural and functional synaptic plasticity in vivo," Eur. J. Pharmacol. **719**(1-3), 128–136 (2013).
5. D. Margolis, H. Lütcke, F. Helmchen, B. Weber, and F. Haiss, "Chronic Two-Photon Imaging of Neural Activity in the Anesthetized and Awake Behaving Rodent," in *Optical Imaging of Neocortical Dynamics*, B. Weber, and F. Helmchen, eds. (Humana Press, 2014), pp. 151–173.
6. T. Knöpfel, "Genetically encoded optical indicators for the analysis of neuronal circuits," Nat. Rev. Neurosci. **13**(10), 687–700 (2012).

#244279 Received 3 Jul 2015; revised 24 Sep 2015; accepted 29 Sep 2015; published 21 Oct 2015

7. M. E. Sheffield and D. A. Dombeck, "Calcium transient prevalence across the dendritic arbour predicts place field properties," Nature **517**(7533), 200–204 (2014).
8. A. J. Schain, R. A. Hill, and J. Grutzendler, "Label-free in vivo imaging of myelinated axons in health and disease with spectral confocal reflectance microscopy," Nat. Med. **20**(4), 443–449 (2014).
9. K. A. Nave, "Myelination and support of axonal integrity by glia," Nature **468**(7321), 244–252 (2010).
10. R. J. Zatorre, R. D. Fields, and H. Johansen-Berg, "Plasticity in gray and white: neuroimaging changes in brain structure during learning," Nat. Neurosci. **15**(4), 528–536 (2012).
11. J. Liu, K. Dietz, J. M. DeLoyht, X. Pedre, D. Kelkar, J. Kaur, V. Vialou, M. K. Lobo, D. M. Dietz, E. J. Nestler, J. Dupree, and P. Casaccia, "Impaired adult myelination in the prefrontal cortex of socially isolated mice," Nat. Neurosci. **15**(12), 1621–1623 (2012).
12. R. J. Franklin and C. Ffrench-Constant, "Remyelination in the CNS: from biology to therapy," Nat. Rev. Neurosci. **9**(11), 839–855 (2008).
13. L. Bø, C. A. Vedeler, H. I. Nyland, B. D. Trapp, and S. J. Mørk, "Subpial demyelination in the cerebral cortex of multiple sclerosis patients," J. Neuropathol. Exp. Neurol. **62**(7), 723–732 (2003).
14. G. Feng, R. H. Mellor, M. Bernstein, C. Keller-Peck, Q. T. Nguyen, M. Wallace, J. M. Nerbonne, J. W. Lichtman, and J. R. Sanes, "Imaging neuronal subsets in transgenic mice expressing multiple spectral variants of GFP," Neuron **28**(1), 41–51 (2000).
15. L. Silvestri, A. L. Allegra Mascaro, I. Costantini, L. Sacconi, and F. S. Pavone, "Correlative two-photon and light sheet microscopy," Methods **66**(2), 268–272 (2014).
16. A. Bria and G. Iannello, "TeraStitcher - a tool for fast automatic 3D-stitching of teravoxel-sized microscopy images," BMC Bioinformatics **13**(1), 316 (2012).
17. A. Bria, G. Iannello, and H. Peng, "An Open-Source Vaa3D Plugin for Real-Time 3D Visualization of Terabyte-Sized Volumetric Images.," in *Procs. of 2015 IEEE Int. Symp. on Biomedical Imaging.*(2015), pp. 520–523.
18. J. Binding, J. Ben Arous, J. F. Léger, S. Gigan, C. Boccara, and L. Bourdieu, "Brain refractive index measured in vivo with high-NA defocus-corrected full-field OCT and consequences for two-photon microscopy," Opt. Express **19**(6), 4833–4847 (2011).
19. I. Costantini, J. P. Ghobril, A. P. Di Giovanna, A. L. Allegra Mascaro, L. Silvestri, M. C. Müllenbroich, L. Onofri, V. Conti, F. Vanzi, L. Sacconi, R. Guerrini, H. Markram, G. Iannello, and F. S. Pavone, "A versatile clearing agent for multi-modal brain imaging," Sci. Rep. **5**, 9808 (2015).
20. T. Ragan, L. R. Kadiri, K. U. Venkataraju, K. Bahlmann, J. Sutin, J. Taranda, I. Arganda-Carreras, Y. Kim, H. S. Seung, and P. Osten, "Serial two-photon tomography for automated ex vivo mouse brain imaging," Nat. Methods **9**(3), 255–258 (2012).
21. I. Blümcke, M. Thom, E. Aronica, D. D. Armstrong, H. V. Vinters, A. Palmini, T. S. Jacques, G. Avanzini, A. J. Barkovich, G. Battaglia, A. Becker, C. Cepeda, F. Cendes, N. Colombo, P. Crino, J. H. Cross, O. Delalande, F. Dubeau, J. Duncan, R. Guerrini, P. Kahane, G. Mathern, I. Najm, C. Ozkara, C. Raybaud, A. Represa, S. N. Roper, N. Salamon, A. Schulze-Bonhage, L. Tassi, A. Vezzani, and R. Spreafico, "The clinicopathologic spectrum of focal cortical dysplasias: a consensus classification proposed by an ad hoc Task Force of the ILAE Diagnostic Methods Commission," Epilepsia **52**(1), 158–174 (2011).
22. J. Dammers, L. Breuer, M. Axer, M. Kleiner, B. Eiben, D. Grässel, T. Dickscheid, K. Zilles, K. Amunts, N. J. Shah, and U. Pietrzyk, "Automatic identification of gray and white matter components in polarized light imaging," Neuroimage **59**(2), 1338–1347 (2012).
23. A. L. Allegra Mascaro, L. Silvestri, L. Sacconi, and F. S. Pavone, "Towards a comprehensive understanding of brain machinery by correlative microscopy," J. Biomed. Opt. **20**(6), 061105 (2015).
24. C. E. Brown, P. Li, J. D. Boyd, K. R. Delaney, and T. H. Murphy, "Extensive turnover of dendritic spines and vascular remodeling in cortical tissues recovering from stroke," J. Neurosci. **27**(15), 4101–4109 (2007).

1. Introduction

In vivo two-photon fluorescence (TPF) imaging is now extensively used for attaining critical insights into brain plasticity. The fluorescence emission from a variety of indicators, either exogenous or genetically encoded, has been widely exploited to monitor structural modification [1–4] and functional activation [5–7] of neurons in a multitude of experimental paradigms. The use of genetically encoded fluorescent indicators is nevertheless limited to a few animal models, and cannot be applied to humans. In addition, since the combination of fluorescent transgenic mice and animal models of pathology requires complex genetic engeneering proceedures, the study of many diseases with fluorescence microscopy is limited. Back-scattered photons from the near-infrared (NIR) laser, usually not collected, carry precious and complimentary information on the brain. As such, additional features might indeed be gained from brain samples without introducing any exogenous labelling. Recently, visible back-scattered photons have been collected to study myelinated axons in live brain [8]. Myelin, which plays a critical role in action-potential propagation, axonal insulation and trophic support [9], is a site of experience-dependent neural plasticity [10, 11]. Axonal demyelination has been demonstrated to be a crucial pathological event in many diseases of the nervous system like multiple sclerosis [12, 13]. Here we show simple implementation of

#244279 Received 3 Jul 2015; revised 24 Sep 2015; accepted 29 Sep 2015; published 21 Oct 2015

the two-photon microscope allow imaging different types of scattering sources such as axonal branches and cells flowing inside blood vessels. We first visualize axonal elongations in fixed brain preparation to dissect morphological features of axonal bundles within the hippocampus. Then we show that axons can be imaged longitudinally under a cranial window in vivo. In addition, this complimentary technique allows monitoring the blood flow velocity in real time without the need of introducing exogenous dyes. This imaging modality could be used in many pathologies involving the degeneration of neurons and oligodendrocytes, the myelin-producing cells, but also of blood flow interruption and angiogenesis. We applied it to a mouse model of cortical stroke to study demyelination and neuronal degeneration dynamics *in vivo* in parallel.

2. Materials and methods

2.1 Setup

As shown in Fig. 1, a mode locked Ti:Sapphire laser (Chameleon, Coherent, CA) is coupled into a scanning system based on a pair of galvanometric mirrors (VM5001, Cambridge Technologies, MA). The laser beam is then expanded by a telescope comprised of a scanning lens (SL) and a microscope tube lens (TL). An objective lens (Zeiss LD C-APOCROMAT 63x/1.15 w) focuses the beam onto the specimen. The system is equipped with a motorized xy stage (MPC-200, Sutter Instrument, CA) for radial displacement of the sample and with a closed-loop piezoelectric stage (ND72Z2LAQ, Physik Instrumente, Germany) for the displacement of the objective along the z-axis. Fluorescence light is separated from the laser optical path by a first dichroic beam splitter (DM1) positioned as close as possible to the objective lens (non-de-scanning mode). A two-photon florescence cut-off filter (720 SP) eliminates reflected laser light. A second dichroic mirror (DM2) is used to split the two spectral components of the fluorescence signal: 510/42 and 630/69 displayed in pseudocolor with green and cyan respectively. The fluorescence signals are collected by two orthogonal photomultiplier modules (H7422P, Hamamatsu Photonics, NJ).

The back-scattered light is collected in de-scanning mode: a polarizing beam splitter (PBS) cube coupled to a quarter wave-plate is placed between the Ti:Sapphire laser and the scanning head to separate the back-scattered component from the excitation path. The horizontally polarized laser light passes through the PBS and is transformed in left-handed circularly polarized light by the quarter wave-plate. The right-handed circularly polarized back-scattered light is then reflected by the PBS and focused into a pinhole (PH) placed in a plane conjugated with the objective focal point. The back-scattered excitation light is finally focalized and collected by an avalanche photodiode (APD; SPCM-AQR-14, Perkin Elmer). An excitation wavelength of 920 nm is used for all experiments. The instrument was controlled by custom software, written in LabVIEW 2010 (National Instruments, TX).

#244279 Received 3 Jul 2015; revised 24 Sep 2015; accepted 29 Sep 2015; published 21 Oct 2015

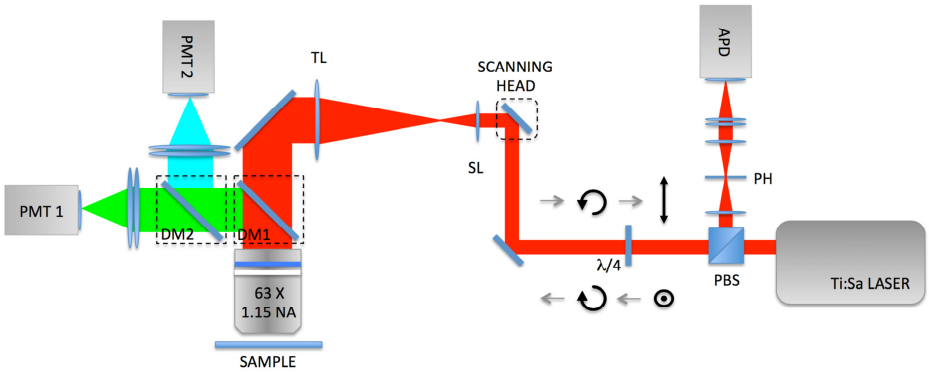

Fig. 1. Custom-made NIR confocal reflectance combined with two-photon fluorescence apparatus. The figure shows the NIR laser light (in red) that is first scanned by two galvanometric mirrors (scanning head), then expanded by a telescope (SL and TL), and finally focused by the objective onto the specimen. The emitted light is separated from the exciting beam by a first dichroic mirror (DM1) and then split by a second dichroic mirror (DM2). Two photomultipliers detect the split fluorescence emissions (PMT1 and PMT2). A polarization beamsplitter (PBS) along with a quarter waveplate is used to direct the descanned reflectance confocal signals to an avalanche photodiode (APD) module with a point spread function size pinhole (PH) in front. The black arrows highlight the status of polarization light in forward and backward direction.

2.2 Sample preparation for ex vivo imaging

An adult (P56) Thy1-GFP-M mouse [14] was deeply anesthetized with an intraperitoneal injection of ketamine (90 mg/kg) and xylazine (9mg/kg). Then it was transcardially perfused with 100 ml of ice-cold 0.01 M phosphate buffered saline (PBS) solution (pH 7.6), followed by 100 ml of freshly prepared ice-cold paraformaldehyde (PFA) 4% in 0.01 M PBS (pH 7.6).

The brain was extracted from the skull and fixed overnight in 20 ml of PFA 4% at 4 °C. It was then rinsed three times (30 minutes each) in 20 ml of 0.01M PBS at 4°C. The hippocampus was manually dissected and embedded in 4% agarose in 0.01 M PBS. Coronal vibratome sections were collected (Vibratome 1000 Plus, Intracel LTD, UK) before imaging.

2.3 Sample preparation for in vivo imaging

A cranial window was inserted in a 12 month old Thy1-GFP-M mouse [14] overlying the somato-sensory cortex. The procedure followed our previous works [2, 15] with slight modifications. Mice were deeply anesthetized by intraperitoneal injection of zooletyl (50 mg/kg) and xylazine (9 mg/kg). A small dose of dexamethasone (0.04 ml at 2 mg/ml) was administrated to minimize swelling at the site of surgery. A circular portion of the skull (5 mm of diameter) above the somato-sensory cortex was removed and the exposed region was then covered with a coverglass and sealed with dental cement. The mice were treated daily with carprofen (5 mg/kg). For fluorescent myelin labelling, Fluoromyelin (F34652, Life Technologies) was diluted to a 50% concentration in PBS, and applied directly on the cortex during surgery. After 45 minutes of incubation, the dye was repeatedly washed and the cranial window was applied. The photothrombotic stroke was performed by illuminating the selected area of the cortex with focused white light for 15 minutes, starting 5 minutes after i.p. injection of Rose Bengal (10 mg/mL). The experimental protocols were designed in accordance with the rules of the Italian Minister of Health.

2.4 Image processing

Acquired imaged stacks were analyzed using ImageJ/Fiji open-source software (http://fiji.sc/Fiji). The coronal section of hippocampus consisted in 40 × 40 tiles, each composed by 768(x) × 768(y) × 6(z) RGB stack of images, which yielded a data set of

#244279 Received 3 Jul 2015; revised 24 Sep 2015; accepted 29 Sep 2015; published 21 Oct 2015

approximately 17 GVoxels. Stitching was therefore performed using TeraStitcher [16], a 3D stitching tool specifically designed to deal with very large images acquired with motorized microscopes that provide reliable nominal tile positions. TeraStitcher 1.9.2 was used, which is able to process multi-channel images. The tiles alignment algorithm was applied to the red channel, which was the one containing enough information for alignment. Then both red and green channels of the stitched image were generated. The reconstructed 3D image consisted of six slices of approximately 25,000 × 25,000 pixels, that were saved in the multiresolution tiled format supported by TeraStitcher for visualization with Vaa3D-Terafly [17].

3. Results

A custom-made two-photon microscope was modified in order to collect backscattered (BS) NIR photons. As depicted in Fig. 1, the horizontally polarized NIR light of the Ti:Sapphire laser is first circularly polarized (left handed) by a quarter waveplate. The right handed BS NIR photons become vertically polarized after passing through the quarter waveplate and are deflected by a PBS (see Material and Methods). They are then focused into a pinhole (PH) placed in a plane conjugated with objective focal point and collected by an avalanche photodiode (APD). We aligned the BS detection path in order to have a colocalization of the TPF and BS focuses with a precision below 500 nm along the z-axis. The pinhole size was chosen in order to match the BS and TPF point spread function (data not shown).

We first applied this combined imaging modality to an hippocampal slice of a Thy1-GFPM mouse brain, in which GFP is expressed in a subset of pyramidal neurons [14]. The BS signal appeared as patchy filaments, reminiscent of axonal elongations. Indeed, the NIR reflectance signal occasionally colocalised with GFP labeled axons, but was never colocalized with neuronal cell bodies or dendrites. (Fig. 2). In agreement with this observation, the reflection signal may be due to changes in refractive index between the aqueous neural tissue and the lipid-rich myelin [18], analogous to a thin-film interference effect.

#244279 Received 3 Jul 2015; revised 24 Sep 2015; accepted 29 Sep 2015; published 21 Oct 2015

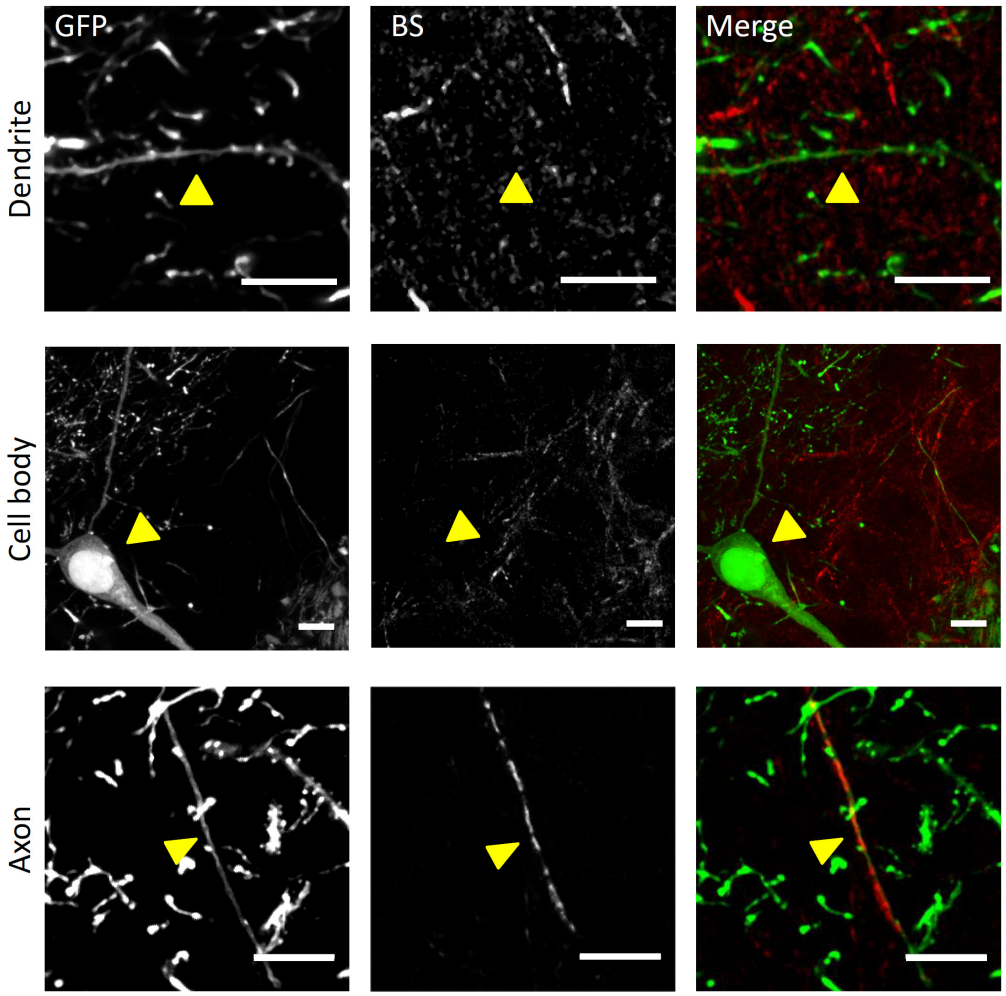

Fig. 2. *Ex vivo* BS NIR and two-photon fluorescence imaging. Ex vivo maximum intensity projection (MIP) of stacks (depth = 10 µm) showing the fluorescence and BS NIR signals in a Thy1-GFPM mouse hippocampus. In the upper panel there is a non-reflective GFP-labeled dendrite (arrowhead). Cell bodies (in the middle panel) are also non-reflective. Axons (lower panel) can be both fluorescent and reflective. From left to right: GFP fluorescence, reflectance, merge with GFP in green and reflectance in red. Scale bar, 10 µm.

We used NIR reflectance to perform a large area reconstruction of a slice of hippocampus from a Thy1-GFPM mouse. Single stacks (10 µm thick, field of view 90 × 90 μm^2) were acquired at 920 nm. The BS signal from axons could be visualized up to 120 µm deep inside the sample. The images were then automatically stitched with the TeraStiticher tool [16]. This large-scale reconstruction shows the presence of regions where large bundles of axons extending over the entire hippocampal slice could be resolved with subcellular resolution. The density of this network of irregular lines varied depending on the anatomical location inside the hippocampus. These tracks and their irregular distribution highlight different regions characteristic of hippocampal anatomy, e.g. dentate gyrus (DG), entorhinal cortex (EC), and *Cornu Ammonis* (CA) regions (Fig. 3).

#244279 Received 3 Jul 2015; revised 24 Sep 2015; accepted 29 Sep 2015; published 21 Oct 2015

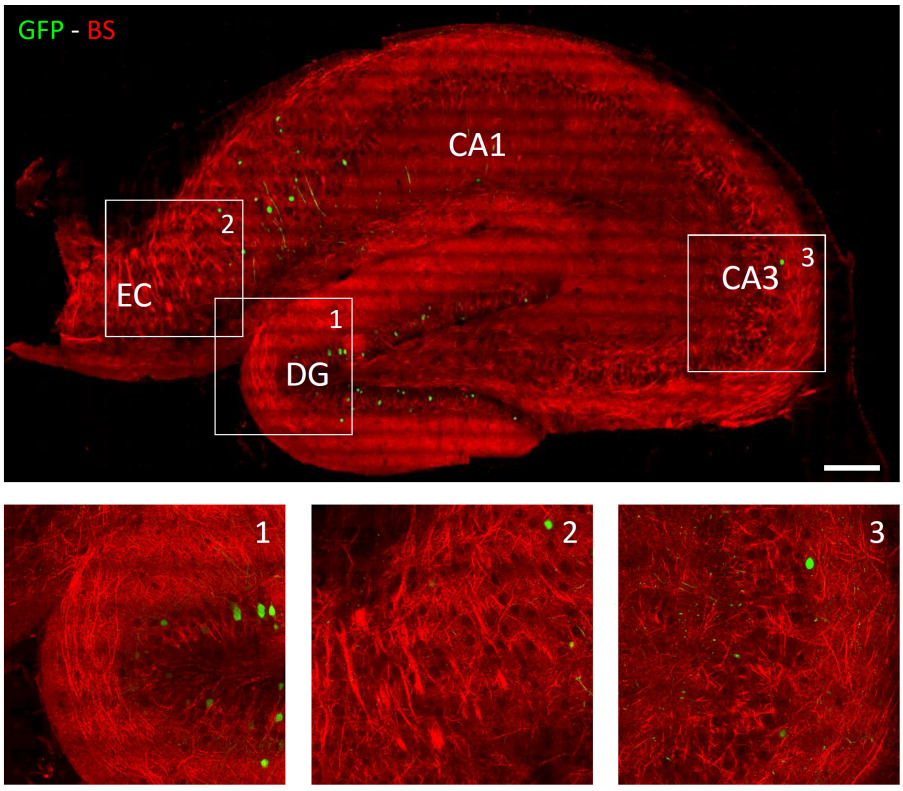

Fig. 3. Thy1-GFPM mouse hippocampus imaging. Reconstruction of a coronal slide of a Thy1-GFPM mouse hippocampus fixed with PFA: in red there is the reflectance signal, in green the fluorescence signal. The upper panel shows the rendering of maximum intensity projection (MIP, depth = 5 µm) of stacks stitched together to reconstruct the entire coronal slide. Scale bar = 100 µm. (1, 2, 3) High magnification inset corresponding to white boxes in the upper panel highlighting the different organization of axonal fibers in the hippocampal areas DG, EC and CA3.

We then explored the potential of this technique in the *in vivo* mouse brain. We imaged a Thy1-GFPM mouse through a cranial window. We could visualize the reflectance signal coming from randomly oriented filaments elongating up to 100 µm deep inside the cortex. Figure 4(a) shows a small 4 × 4 mosaic of stitched maximum intensity projections from 60 µm deep stacks. As in *ex vivo* measures, GFP expressing axons occasionally colocalized with the patchy patterns of the BS signal. Even though myelin is supposed to be the main source of reflectance [8], the reflective network pattern we observed is mainly composed of fragmented lines.

#244279 Received 3 Jul 2015; revised 24 Sep 2015; accepted 29 Sep 2015; published 21 Oct 2015

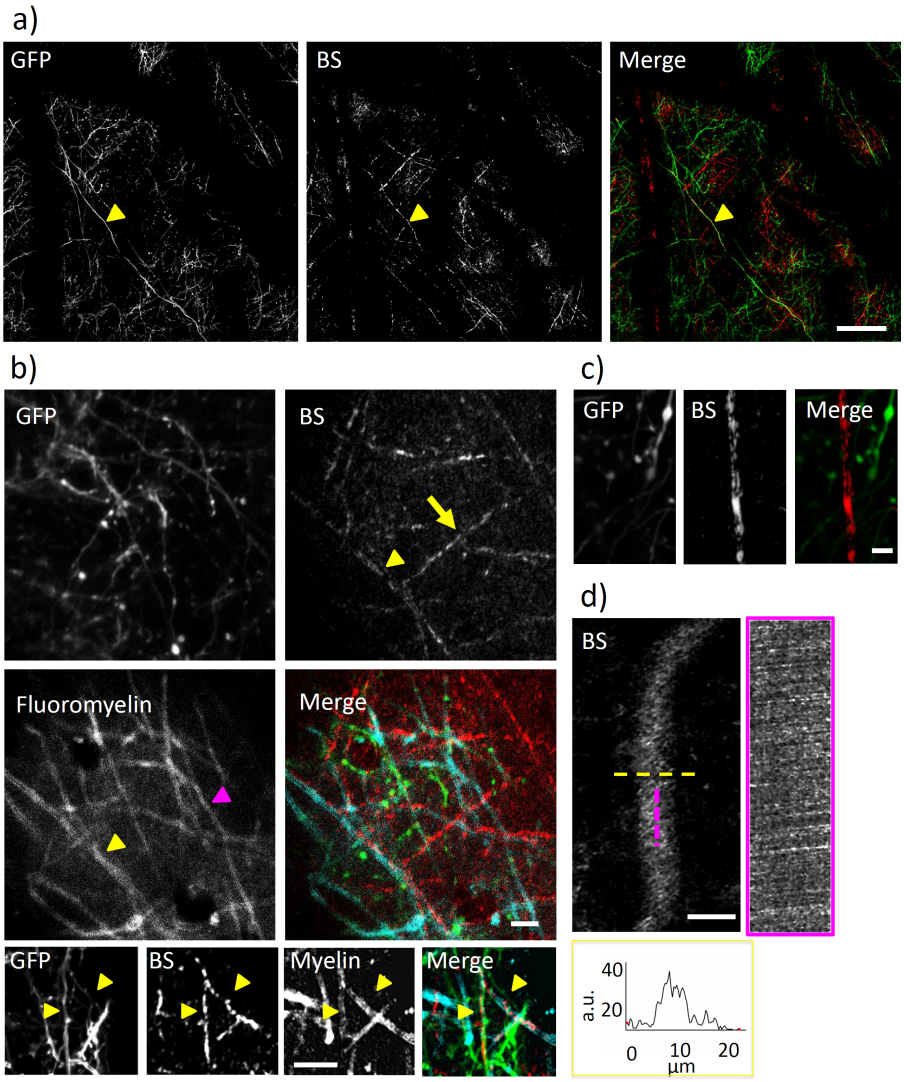

Fig. 4. In vivo NIR reflectance and two-photon fluorescence imaging. a) Mosaic of 4 × 4 maximum intensity projections from 60 µm deep stacks (90 × 90 µm wide, 10 µm overlap between the stacks). Colocalization of an axon in the fluorescence and BS channel, as pointed out by the arrowhead. Scale bar, 50 µm. b) Upper panels are MIP of TPF and BS images showing the possible colocalization of the BS signal with Fluoromyelin labeling (as highlighted by the yellow arrowhead). Yellow arrow points at a BS filament not colocalized with Fluoromyeling signal. The magenta arrowhead highlights a Fluoromyelin labeled axon which is not visible in the BS channel. Scale bar, 20 µm. Lower panels show an example of colocalization of NIR reflectance signal (BS) with GFP fluorescence and with Fluoromyelin labeling on the same axons (highlighted by yellow arrowheads). c) MIP of TFP and BS images where a binary of reflectance signal shows the sides of the myelinated tube. d) Blood capillary as visualized by NIR reflectance imaging. By performing line scans along the magenta and yellow line, we could measure blood flow velocity and lumen diameter (respectively) from the NIR reflectance signal. The graph on the right reports the profile of BS signal measured by the line scan (yellow line) on the blood vessel. Unless otherwise stated, scale bar = 10 µm.

To confirm that the reflectance signal originated from myelinated axons (as suggested in [8]), we used the dye Fluoromyelin, applied on the cortex. Figure 4(b) (lower panels) shows the colocalization of the reflectance signal with GFP fluorescence and with Fluoromyelin labeling on the same axon. Even though most of the Fluoromyelin labeled axons showed

#244279 Received 3 Jul 2015; revised 24 Sep 2015; accepted 29 Sep 2015; published 21 Oct 2015

corresponding signals in the BS channel (Fig. 4(b), yellow arrowheads), we sporadically detected BS filaments that did not colocalized with Fluoromyelin signal (Fig. 4(b), yellow arrow) and viceversa (Fig. 4(b), magenta arrowhead). In addition, we occasionally saw binaries of reflectance signal, where the signal probably derives from the sides of the myelinated tube (Fig. 4(c)), similar to the fluorescence labeling obtained with Fluoromyelin.

We observed that the reflectance signal originated also from rapidly flowing cells inside blood vessels. By performing repeated line scans along the vessel, we could measure blood flow velocity and lumen diameter from the NIR reflectance signal (Fig. 4(d)).

We showed that the NIR reflectance technique could highlight important features of hemodynamic and neuronal features without any exogenous labeling. We thought it would be a perfect tool to study the effect of neuronal degeneration caused by interruptions in blood flow. Therefore, we applied a photothrombotic model of cortical stroke to investigate the effect of blood clotting and hemorrhage on axonal myelination. We irradiated the motor cortex of a Thy1-GFPM mouse for 15 minutes after i.p. injection of a 10 mg/ml solution of Rosa Bengal. We repeatedly imaged the cortex adjacent to the injury site through the cranial window. In the hours that followed the irradiation, we observed increasing blebbing and degeneration of the GFP-labeled axons and dendrites. In parallel, some of the axons undergoing progressive swelling (Fig. 5, upper panels, yellow arrowhead) showed BS signal colocalization on spared regions of the axon, possibly indicating the retention of the myelin ensheathing.

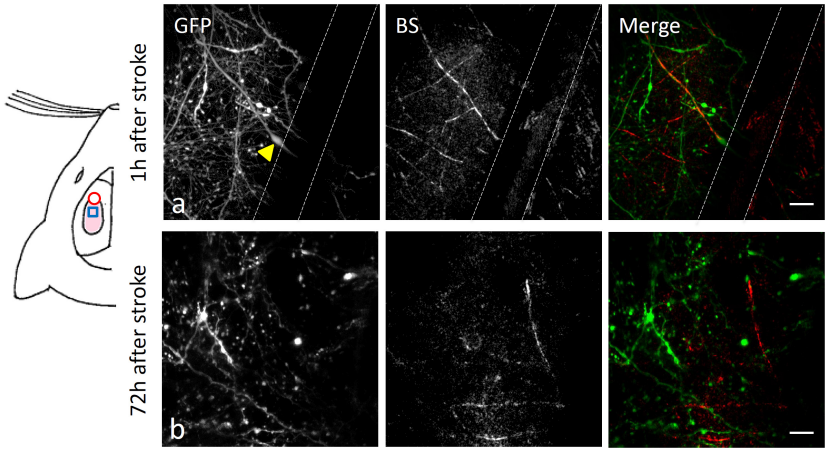

Fig. 5. In vivo imaging of NIR reflectance after stroke. On the left, a cartoon of a mouse head illustrate the relative position of the craniotomy (light pink area), the stroke core (red circle) and the imaging region (blue square). Upper panels show the retention of the BS signal in an axon partially degenerated one hour after producing a photothrombotic stroke. The yellow arrowhead points at a swelled region of a partially degenerated axon. The dashed white lines highlight the presence of a blood vessel. Lower panels show axonal elongations detected by NIR reflectance imaging in the peri-infarct area 72 hours after stroke. Scale bar, 10 μm.

Three days after stroke, there were still widespread swellings of fluorescent structures in the immediate proximity (≤ 300 μm) of the irradiated area. In these regions, we could still detect some BS lines from NIR reflectance imaging (Fig. 5, lower panels). Nearer to the stroke region, there were fewer fragments of BS signals. Further from the damage site (≥ 300 μm), the distribution of BS lines was similar to what we described in control conditions.

4. Discussion

The system we proposed here allows imaging axons in fixed preparation and in murine cortex *in vivo* by a simple implementation of the two-photon microscope. A recent paper by Shain et al. [8] described the use of visible laser light to perform imaging of myelin inside living mouse brain. In the present study we propose to complement the data obtained with two-

#244279 Received 3 Jul 2015; revised 24 Sep 2015; accepted 29 Sep 2015; published 21 Oct 2015

photon fluorescence imaging with the information on axonal structures and hemodynamic features within the cortex. This complimentary information can be gained by collecting the backscattered NIR photons via simple modifications of an existing two-photon microscope. The only critical point in the setup of this technique is the precise alignment of the BS and TPF foci along the z axis, which requires micrometric-precision 3D stages for beam positioning. The proposed implementation of a two-photon system is cost-effective and easy; all the components are commercially available.

As suggested in [8], myelin is supposed to be the source of reflectance. In agreement with this hypothesis, NIR reflectance showed that the BS signal might come from the sides of the axonal myelinated tube, as seen with Fluoromyelin labelling. However, the BS signal in the *xy* plane mostly generated from the center of the myelinated tube as observed in [8].

By performing Fluoromyelin labeling of cortical neurons, we showed that the colocalization with the BS signal is extensive but not exhaustive. Few myelinated axons do not show BS signal, and Fluoromyelin labels not all the BS filaments. The possible lack of colocalization of Fluoromyelin and BS signals suggests that either myelin is not the exclusive source of BS or Fluoromyelin does not label all the myelinated axons. Although the precise mechanism for NIR reflection is not clear, it probably relates to the principle of thin-film interference [8]. Similar to dichroic mirrors with alternating layers of optical coatings of different refractive indices, the interfaces between lipid-rich sheaths of myelin and water might be the origin of the reflection. Anyhow, an exhaustive explanation of the origin of the NIR BS signal would require *ad hoc* investigation.

We showed that we could perform a large-scale reconstruction of a hippocampal slice. NIR reflectance could be used in combination with serial two-photon microscopy [19, 20] for mapping axonal projections over large regions, like the entire hippocampus. The BS signal also helped in recognizing characteristic anatomical features of the tissue, thus making it a useful tool for brain atlassing. This could be extremely useful in human biopsies, possibly in parallel with other large scale imaging techniques. In human brain samples, NIR reflectance could be indeed fundamental in retrieving critical features of axonal demyelination or of layer dyslamination pathologies (for example Focal Cortical Dysplasia [21]), without the need of exogenous labeling. NIR reflectance imaging could be further used as validation tool for other techniques like, for example, polarization light microscopy [22]. Moreover, the possibility of retrieving similar features on *in vivo* and *ex vivo* preparations facilitates the registration of images acquired with different modalities in correlative studies [15, 23].

In this work, NIR reflectance was applied to monitor the presence of axons in the peri-infarct regions. NIR reflectance could also be applied to monitor axonal rearrangement (similar to what has been observed in [24], but without the need of fluorescence labeling) and progressive demyelination after stroke. This imaging modality could also provide new details on the timeline and the mechanism of myelin disruption in axonal degeneration.

NIR reflectance imaging is a complimentary label-free imaging modality that could be used in combination with two-photon microscopy for the study of many pathologies that encompass the degeneration of neurons and myelination pathologies but also alterations in hemodynamics processes and angiogenesis.

Acknowledgments

This research has received funding from LASERLAB-EUROPE (grant agreements no. 284464, 7's Seventh Framework Programme) and has been supported by the Italian Ministry for Education, University and Research in the framework of the Flagship Project NANOMAX. This work has been supported by Regione Toscana in the framework of POR-CreO 2007-2013 action (SMAG project). This work has been supported by "Ente Cassa di Risparmio di Firenze. The research leading to these results has received funding from the European Union Seventh Framework Programme (FP7/2007-2013) under grant agreement no. 604102 (Human Brain Project). Part of this work was performed in the frame of the Proof of Concept Studies for the ESFRI research infrastructure project Euro-BioImaging at the PCS facility LENS.

#244279 Received 3 Jul 2015; revised 24 Sep 2015; accepted 29 Sep 2015; published 21 Oct 2015